Hydrogen chemisorption on Si(111)7×7 studied with surface-sensitive core-level spectroscopy and angle-resolved photoemission

C. J. Karlsson, E. Landemark, and L. S. O. Johansson
Department of Physics and Measurement Technology, Linköping Institute of Technology, S-58183 Linköping, Sweden

U. O. Karlsson
Max-lab, Box 118, University of Lund, S-22100 Lund, Sweden

R. I. G. Uhrberg
Department of Physics and Measurement Technology, Linköping Institute of Technology, S-58183 Linköping, Sweden
(Received 31 July 1989)

Photoelectron spectroscopy of the Si 2*p* core level has been performed in order to determine surface core-level shifts for the Si(111)"7×1":H and Si(111)7×7 surfaces, as well as to determine the Fermi-level position in the bulk band gap for the "7×1":H surface. Angle-resolved ultraviolet photoelectron spectroscopy has been used to determine the initial energy versus *k*-parallel dispersion for the surface state on the hydrogen-exposed surface. The results of these measurements imply that the monohydride phase is formed within the 7×7 unit cell after the hydrogen exposure. The core-level spectroscopy results obtained for the 7×7 surface are in good qualitative agreement with earlier results, but we suggest, in contradiction to a previous interpretation, that the surface component which shifted to lower binding energy corresponds to the rest atoms and not to the adatoms.

I. INTRODUCTION

When the Si(111)7×7 surface is exposed to activated hydrogen the low-energy electron diffraction (LEED) pattern transforms to a "7×1" pattern, which indicates a substantial rearrangement of the atomic structure. The resulting surface exhibits several similarities with the monohydride phase of the hypothetical Si(111)1×1:H surface,[1] considering, e.g., the surface-state dispersion. In the monohydride phase each dangling bond on the ideal 1×1 surface is saturated by a hydrogen atom. The H-exposed surface has been studied for several years with many different techniques, e.g., ultraviolet photoelectron spectroscopy (UPS),[2–5] LEED,[6,7] reflection high-energy electron diffraction (RHEED),[8] electron-energy-loss spectroscopy,[2,9] and infrared spectroscopy.[10] Even though the Si(111)"7×1":H surface has been studied quite a lot, the answer to the central question about whether the monohydride and/or the dihydride and/or the trihydride phase is formed, still remains unclear. From the UPS studies (Refs. 3–5) it was concluded that the monohydride phase is formed at low hydrogen coverages. Pandey[1] concluded that the trihydride phase is formed after high coverages on the "quenched 1×1" surface. Recently a RHEED intensity analysis[8] of the hydrogen exposed surface suggested the trihydride phase and an EELS study (Ref. 9) indicated that the dihydride and/or the trihydride phase is formed even at low coverages.

Our angle-resolved photoelectron spectroscopy (ARPES) measurements indicate that the monohydride phase is formed on the Si(111)"7×1":H surface, obtained by hydrogen exposure of the Si(111)7×7 surface. Two main features are seen in the spectra, centered around 5.6 and 7.6 eV below the Fermi level (E_F). The structure centered around −5.6 eV corresponds to emission from the surface state due to the Si—H bond, and the −7.6 eV structure corresponds to a direct bulk transition. The dispersion of the hydrogen-induced surface state has been mapped out along the main directions in the 1×1 surface Brillouin zone (SBZ). The experimental dispersion is similar to the surface-state dispersion for the monohydride phase as calculated by Pandey.[1]

Measurements of the Si 2*p* core level have been done for the Si(111)7×7 and the Si(111)"7×1":H surfaces. From these data, surface core-level shifts and Fermi-level positions are determined. The result obtained for the "7×1":H surface confirms the interpretation of the ARPES spectra, i.e., the monohydride phase is formed within the 7×7 unit cell. The surface core-level shifts, obtained in this study, for the 7×7 surface are in good agreement with previously determined surface core-level shifts.[11] We present, however, a different interpretation of the origin of the surface shifted components, based on the dimer adatom stacking-fault (DAS) model[12] (shown in Fig. 1 from Ref. 13) for the 7×7 surface.

II. EXPERIMENTAL DETAILS

The experiments were performed at the toroidal grating monochromator beam line[14] at the MAX synchrotron radiation facility in Lund, Sweden. Both the ARPES and the core-level measurements were performed in standard UHV chambers with base pressures of $\approx 2\times10^{-10}$ Torr. The ARPES spectra were recorded with a hemispherical analyzer and the core-level spectra with a double-pass cylindrical-mirror analyzer (CMA). The CMA accepts electrons with emission angles in the interval 36°–48° if the CMA axis is parallel to the surface normal. The

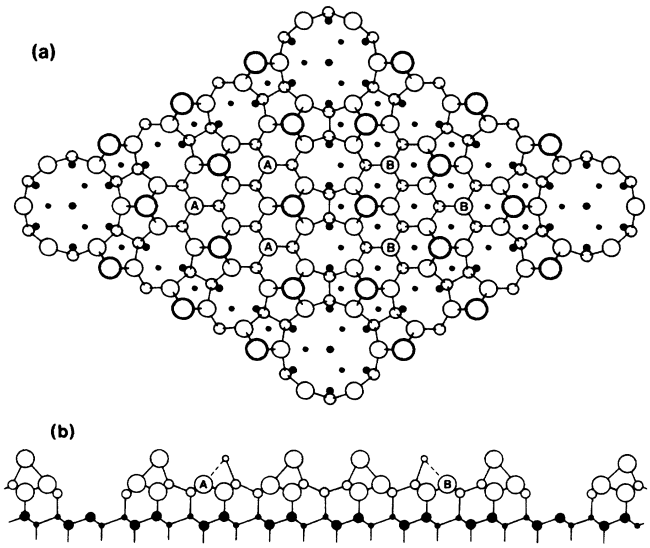

FIG. 1. DAS model of Takayanagi *et al.* (Ref. 12), from Ref. 13. (a) Top view. Atoms in (111) layers at increasing depths are indicated by circles of decreasing sizes. Adatoms are shown by heavily outlined shaded circles, rest atoms are shown with circles marked *A* and *B* to indicate rest atoms in the faulted and unfaulted halves of the 7×7 unit cell, respectively. The small, shaded circles represent the dimer atoms. (b) Side view *A* cut along the long diagonal of the 7×7 unit cell. Atoms that are behind this cut are shown with smaller circles than those along the diagonal.

spectra in this study were obtained with the CMA axis 30° off the surface normal, which implies that a wide range of emission angles are probed.

The Si(111) samples were preoxidized with an etching method[15] and cleaned *in situ* by direct current heating at 850 °C. This procedure resulted in a clean and well-ordered surface, as evidenced by the strong surface-state emission and a sharp 7×7 LEED pattern. Samples of two different doping levels were used, n:(2–10) Ω cm (phosphorus) and n^+:(4–6) m Ω cm (arsenic), in order to determine quantitative effects on the Fermi-level pinning at the 7×7 surface due to different doping levels. The ARPES spectra and the core-level spectra were recorded at different occasions. The spectral features of the valence band and the Si 2*p* core level, as well as the LEED pattern, were well reproduced in the two studies, which ensures that the two measurements were performed on identical surfaces.

The hydrogen exposures were done with the samples facing a hot (≈1700 °C) tungsten filament for 60 s at a hydrogen pressure of $\approx 1.6\times10^{-5}$ Torr. Thus the surfaces were subject to a total exposure of ≈1000 L [1 L (langmuir) $\equiv 1\times10^{-6}$ Torr s]. After the exposure, the samples used for the measurements of the Si 2*p* core level were annealed to ≈400 °C. The sample used for the ARPES measurement was prepared according to the above-described procedure, though without any anneal. The only difference observed in the ARPES data, before and after annealing (≈400 °C), was a change in the Fermi-level position. Stepwise annealing of the samples up to ≈500 °C did not affect the surfaces, but when a temperature of ≈600 °C was reached the LEED pattern transformed to the 7×7 pattern.

III. RESULTS AND DISCUSSION

A. LEED

After the hydrogen exposure of the Si(111)7×7 surface, all the seventh-order diffraction spots of the clean surface disappeared except those lying on the lines joining the 1×1 spots. The pattern thus appears like a three domain 7×1 pattern. The transformation of the 7×7 pattern occurs gradually at room-temperature exposure and the surface persists in showing seventh-order diffraction spots (those lying on the lines joining the 1×1 spots), until the "7×1" pattern is formed.[3] These facts suggest that the structural change forced by the H exposure involves only a local modification of the 7×7 unit cell. This is consistent with the analysis of the 7×1 pattern done by McRae and Caldwell,[6] who could explain the 7×1 pattern for the H-exposed surface as arising from island arrays where each island is large compared to a 1×1 unit cell and where each island is of local 1×1 periodicity. This analysis, applied to the DAS model of the 7×7 reconstruction, then suggests that a 1×1 hydrogen-terminated surface is formed on the triangular terraces, while the corner holes and the dimer walls may still be present in order to maintain the 7× periodicity.

B. Core-level spectroscopy

Core-level spectra were recorded with photon energies of 108 and 130 eV which results in kinetic energies of ≈4 and ≈26 eV, respectively, for the Si 2*p* electrons [E_B for Si $2p_{3/2}$ = 99.2 eV (Ref. 16) below the valence-band edge]. A kinetic energy of 26 eV corresponds to a very short mean free path and the 130-eV spectra are thus revealing the contribution from the surface layer to the Si 2*p* emission (surface sensitive: SS). The 108 eV spectra are, in analogy, bulk sensitive (BS) due to the long mean free path for electrons of ≈4 eV kinetic energy. Most of the information about the surface is contained in the SS spectra, and we have therefore limited our presentation to displaying those spectra. However, the BS spectra were used to determine certain fitting parameters (described below) and they were also used to check that the binding energies and surface core-level shifts, derived from the fitting procedure, were the same in both BS and SS spectra.

Figure 2 shows SS spectra from the Si 2*p* core level for the Si(111)7×7 and Si(111)"7×1":H surfaces. The spectra were fitted with a nonlinear least-square method[17] using components consisting of convolutions of Gaussian (experimental resolution) and Lorentzian (life-time broadening) functions. Each component is split due to spin-orbit interaction in the final state. The resulting doublet is characterized by the spin-orbit split (energy difference between $2p_{3/2}$ and $2p_{1/2}$) and the branching ratio (intensity ratio between $2p_{1/2}$ and $2p_{3/2}$). The spin-orbit split and the Lorentzian width were constrained to be the same for both the BS and the SS spectra. The

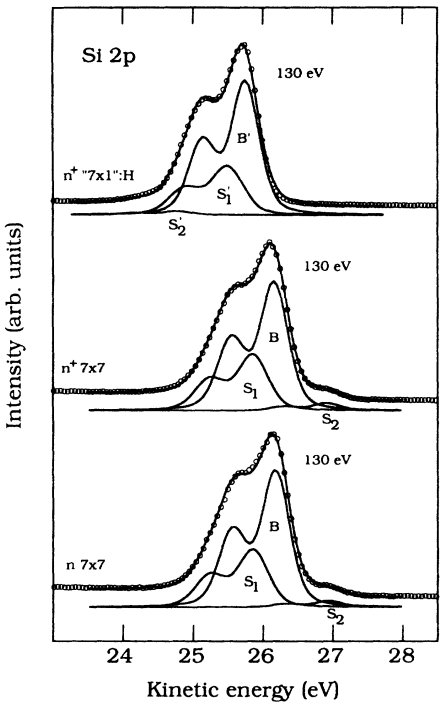

FIG. 2. Core-level spectra for Si(111)7×7 and Si(111)"7×1":H. All three spectra were obtained with a photon energy of 130 eV. The three solid curves show the three components that were used to fit the experimental data (circles). The solid curve through the data shows the resulting fit.

branching ratio and the Gaussian width were allowed to vary between BS and SS spectra due to different final states and different monochromator resolution, respectively. In order to obtain the best fit, we have allowed the Gaussian width in the SS spectra to become larger than the expected experimental width as derived from the analyzer and monochromator resolutions. Possible explanations for the additional width of the components in the SS spectra are discussed below. The fitting parameters are tabulated in Table I as well as the surface core-level shifts and the intensity ratios (described below). A surface core-level shift will be defined as positive if the core-level binding energy for a surface atom is larger than for a bulk atom.

The intensity ratio for a surface component is here defined as the area for that component divided by the area for the bulk component and the second surface component. Defining the intensity ratios in this way makes it possible to do comparisons with intensity ratios calculated according to the following model. Assuming each monolayer attenuates the intensity in an equal degree, one obtains

$$R = \frac{x}{\dfrac{1}{1-e^{-d/\lambda\cos\theta_{\rm cry}}} - x} ,$$

where R is the above-described intensity ratio, d is the average spacing between monolayers (1.57 Å), λ is the mean free path, $\theta_{\rm cry}$ is the emission angle in the crystal, and x is the fraction of surface atoms, contributing to the surface component, compared to a monolayer. In the following calculations of intensity ratios we will use a mean free path of 3.9 Å for the SS spectra. This value for the mean free path was obtained, for a kinetic energy of 26 eV in vacuum, from a study of the Si(111)-Cl surface by Morar *et al.*,[18] by taking the average of the two experimental curves presented. The values for the mean free path for the different energies were calculated in Ref. 18 according to the above-described model with $x = 1$ [1 ML (monolayer) of chemisorbed Cl].

The emission angle in the crystal is related to the emis-

TABLE I. Fitting parameters for the components used to fit the Si 2p core-level spectra shown in Fig. 2. All energies are in eV. The Lorentzian and Gaussian widths refer to the full width at half maximum. The theoretical value for the branching ratio is 0.5. The intensity ratio R is defined in the text. All spectra were fitted with an integrating background.

	Si 2p Si(111)7×7 n doped	Si 2p Si(111)7×7 n^+ doped	Si 2p Si(111)"7×1":H n^+ doped
Spin-orbit split	0.614	0.614	0.614
Lorentzian width	0.15	0.15	0.15
Branching ratio	0.55	0.55	0.54
Bulk component (B)			
Gaussian width	0.38	0.38	0.38
Surface component (S_1,S_1')			
Core-level shift	0.32	0.31	0.26
Gaussian width	0.42	0.42	0.45
Intensity ratio R	0.43	0.44	0.39
Surface component (S_2,S_2')			
Core-level shift	−0.76	−0.76	0.98
Gaussian width	0.38	0.38	0.38
Intensity ratio R	0.033	0.040	0.020

sion angle in vacuum, θ_{vac}, by[19] (to a first approximation)

$$\sin\theta_{cry}=\frac{\sin\theta_{vac}}{\left[1+\frac{V_0}{E_k}\right]^{1/2}},$$

where V_0 is the inner potential, relative to the vacuum level, and E_k is the kinetic energy of the photoelectron in vacuum. A value for the inner potential was derived in an earlier study of direct bulk transitions in silicon.[20] It was shown in that study that the final band could be approximated by a free-electron band using a value of 12.1 eV relative to the valence-band maximum (E_V) for the inner potential. For the Si(111)7×7 and the Si(111)"7×1":H samples this corresponds to inner potentials of ≈17 and ≈18 eV, respectively, relative to the vacuum level. Due to the measurement geometry, the emission angle θ_{cry} is here approximated by the average emission angle inside the crystal. Using the refraction condition and the values derived for the inner potential, we obtain an effective emission angle of 33° for both Si(111)7×7 and Si(111)"7×1":H.

1. *Si(111)7×7*

Our results for the surface core-level shifts on the 7×7 surface are in good qualitative agreement with the results obtained by Miller *et al.*[11] As can be seen in Fig. 2 and Table I the large surface component (S_1) is shifted 0.32 eV for the *n*-doped sample and 0.31 eV for the n^+-doped sample. The small surface component (S_2) is shifted −0.76 eV for both the *n*- and the n^+-doped samples. The fitting parameters are tabulated in Table I.

Scanning tunneling microscopy (STM) of the 7×7 surface reveals 12 bumps, in each unit cell, slightly raised above the mean surface level. Miller *et al.* attributed S_2 to these bumps, i.e., to adatoms. Their assignment was solely based on the different bonding configuration of the adatoms compared to the other surface atoms. Furthermore, they attributed S_1 to the first full monolayer of the 7×7 surface.

Based on the atomic and electronic structure associated with the DAS model[12] of the Si(111)7×7 surface we come to quite different interpretations of the S_1 and S_2 shifts. There are several different types of atoms in this model that could give rise to different core-level binding energies, e.g., adatoms (12), rest atoms (6), atoms binding to the adatoms (36), and dimer atoms (18). It was concluded from a theoretical study[21] of the electronic structure that electrons are transferred from the adatoms to the rest atoms. The result of this charge transfer is a doubly occupied surface state on the rest atoms, at ≈0.8 below E_F, and a surface state close to E_F on the adatoms. The electronic structure obtained by STM (Ref. 22) and ARUPS (Ref. 23) confirms that the charge transfer takes place. Such a charge transfer should, qualitatively, result in a shift to lower binding energy for the rest atoms and a shift to higher binding energy for the adatom core level. This has indeed been suggested for Ge(111)*c*(2×8) (Ref. 24).

The *R* value for S_2 should, according to the above-described model, be ≈0.049 (0.10) if it is the rest atoms (adatoms) that contribute to S_2. The observed *R* values for S_2, ≈0.033 (*n* doped) and ≈0.040 (n^+ doped), are in fair agreement with the rest atom value. Based on the charge-transfer argument and the observed intensity ratio we thus attribute S_2 to the rest atoms. The deviation between the calculated and experimental *R* values, by a factor of 1.23 for the n^+-doped sample (1.48 for the *n*-doped sample), is probably due to the fact that the mean free path is not known exactly and that an effective, average emission angle was used.

From the charge-transfer argument one would, in analogy, expect the S_1 component to correspond to the adatoms. The observed *R* values for S_1 are ≈0.43 (*n* doped) and 0.44 (n^+ doped). These values are significantly larger than the 0.10 expected for the adatoms, and S_1 can thus not correspond to the adatoms alone. In the analysis of the 3*d* core-level spectra from the Ge(111)*c*(2×8) surface, which also show two surface shifted components, the smaller component (S_2) was attributed to the rest atoms and the larger component (S_1) to the adatoms plus the atoms that bind to the adatoms. We will continue the analysis by assuming that S_1 can be assigned to the adatoms plus the atoms that bind to the adatoms (12+36=48 atoms) also for the Si(111)7×7 surface. The calculated intensity ratio for these 48 atoms is 0.60 which should be compared to the observed *R* values of 0.43 and 0.44 for the S_1 component. When these intensity ratios are multiplied by the experimental correction factor 1.23 deduced for the S_2 component we obtain 0.53 and 0.54, respectively (The factor 1.48 gives 0.64 and 0.65, respectively). These corrected *R* values are in close agreement with the calculated value of 0.60, which makes the suggested assignment plausible. As shown by the above analysis it is quite possible to arrive at the same explanation for the S_1 and S_2 surface shifts for both Si(111)7×7 and Ge(111)*c*(2×8). There is, however, a need for a theoretical investigation to verify the assumption that the adatoms and the atoms that bind to the adatoms exhibit a similar surface core-level shift. A second thing that needs to be investigated is the negative surface shift of S_1 on the Ge(111)*c*(2×8) surface.

The fairly large widths of the components in the SS spectra may have a natural explanation in terms of the atomic structure of the DAS model. In an STM study of the 7×7 surface[22] there is a clear difference between the faulted and unfaulted halves when tunneling from the adatom states. This difference in the electronic structure between the two halves may result in slightly different core-level binding energies causing a broadening of the S_1 component. The bulk component in the SS spectra corresponds to atoms very near the surface and they may also be affected by the difference between the faulted and unfaulted halves. The above assignments of S_1 and S_2 imply that the dimer atoms contribute to the bulk component, which is another possible source for a broadening.

The change in kinetic energy of the bulk component monitors the change of the Fermi-level position in the band gap. We have used the SS spectra to determine the Fermi-level shifts, since the very thin band-bending re-

gion for the n^+-doped sample results in an asymmetric broadening of the bulk component in the BS spectrum, which gives an artifical Fermi-level shift. As can be seen in Fig. 2 there is only a very small difference (0.02 eV) in the Fermi-level position between the n^+- and the n-doped sample. This change is of the order of the accuracy of the fitting procedure and the experimental data, and we therefore conclude that the pinning of the Fermi level at the 7×7 surface is the same for both n- and n^+-doped samples. The Fermi-level pinning at the 7×7 surface has been studied in detail by Himpsel *et al.*[25] They determined that the Fermi level is pinned 0.63 eV above the valence-band maximum.

2. *Si(111)"7×1":H*

The 130 eV spectrum for the Si(111)"7×1":H surface is shown in Fig. 2 and the parameters used for the fitting are tabulated in Table I. The most apparent difference between the Si 2*p* core-level spectra for the "7×1":H and the 7×7 surface is that the surface component S_2, here assigned to the rest atoms, now has disappeared. This implies that the rest atoms are highly involved in the structural change forced by the hydrogen exposure, which is in agreement with a previous STM study of NH_3 chemisorption on Si(111)7×7 performed by Wolkow and Avouris.[26] They concluded that the rest atoms are the most reactive atoms on the 7×7 surface with respect to hydrogen. The largest surface component (S_1') shows a surface core-level shift of 0.26 eV and an intensity ratio of ≈0.48, when corrected by the factor 1.23 (0.58 when corrected by 1.48). A surface core-level shift of 0.26 eV has previously been determined for Si atoms bonded to H atoms on the Si(111)1×1:H surface,[27] obtained by exposing the cleaved Si(111)2×1 surface to activated hydrogen. The observed intensity ratio for S_1' is smaller than the value for S_1 on the 7×7 surface. This intensity decrease can qualitatively be explained if the hydrogen atoms displace the adatoms and bind to the terrace atoms. The S_1' component would then correspond to 42 atoms (6 rest atoms plus the 36 atoms that bind to the adatoms on the 7×7 surface) instead of 48 atoms for S_1. The calculated R value for the 42 terrace atoms is ≈0.49 which is in good agreement with the corrected experimental value of 0.48 (0.58). The core-level data then suggest that the monohydride phase is formed on the triangular terraces by simply replacing one adatom with three hydrogen atoms and by saturating each rest atom dangling bond with a hydrogen atom. The fairly large width of the S_1' component may be due to some disorder, which could be explained by the possibility that the saturation coverage is not reached and/or that adatoms still are present with or without chemisorbed hydrogen. However, this larger width could also be explained by different core-level binding energies on the faulted and unfaulted halves. There is also a small surface component (S_2') in the Si 2*p* spectrum for the "7×1":H surface with a shift of 0.98 eV, which may correspond to Si—O or Si—OH bonds,[28,29] i.e., contamination due to oxygen or water chemisorption.

Hollinger and Himpsel[28] concluded that for oxygen chemisorption on Si(111) the surface core-level shift is linearly related to the number of adsorbed oxygen atoms on a Si atom, i.e., one chemisorbed oxygen atom gave a surface core-level shift of 0.9 eV, two gave a shift of 1.9 eV, and three gave a shift of 2.6 eV. For hydrogen chemisorption one could expect, in analogy, a surface core-level shift of ≈0.52 eV for a dihydride phase and a shift of ≈0.78 eV for the trihydride phase. A Madelung-type contribution to the surface core-level shift would spoil this reasoning. However, the above-described linearity is in fact also seen for the monohydride and dihydride phase of the hydrogen-exposed Si(100) surface.[30] Since no surface shifted components are detected at ≈0.52 or ≈0.78 eV we conclude that the monohydride phase is dominating on the Si(111)"7×1":H surface.

As can be seen from Fig. 2, the Fermi-level position changes by 0.43 eV upwards in the gap after exposure and $E_F - E_V$ is thus 1.06 eV for Si(111)"7×1:H, assuming $E_F - E_V = 0.63$ eV (Ref. 25) for Si(111)7×7. The Fermi-level position at the surface is thus almost degenerate with the conduction-band minimum ($E_C - E_V = 1.12$ eV). This is expected for the n^+-doped sample since the H exposure causes the surface states on the 7×7 surface to disappear and thus the Fermi level is no longer pinned at the surface.

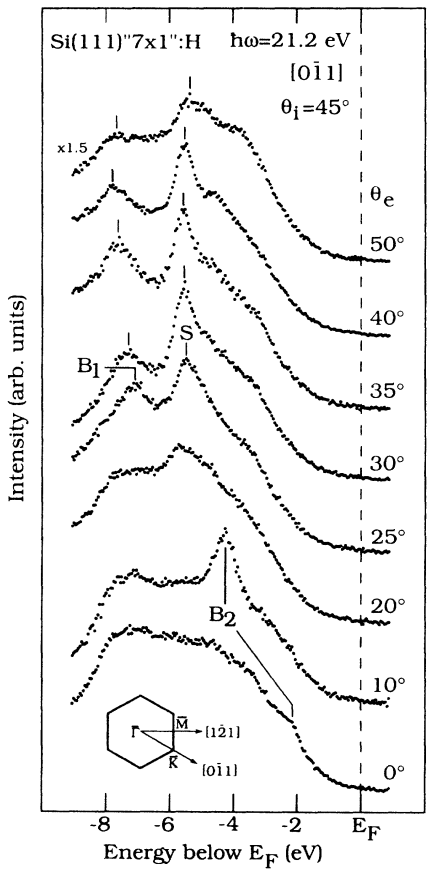

FIG. 3. Photoemission spectra recorded with 21.2 eV photon energy for various angles of emission along the $\bar{\Gamma}$-$\bar{K}$-$\bar{M}$ direction in the 1×1 SBZ. The 1×1 SBZ is shown as an inset.

C. Angle-resolved photoemission

ARPES spectra were recorded in the $\bar{\Gamma}$-$\bar{K}$-$\bar{M}$ and $\bar{\Gamma}$-$\bar{M}$ azimuthal directions in the 1×1 SBZ (see inset in Fig. 3) using 21.2 eV photon energy. The spectra for the two directions are shown for different emission angles in Figs. 3 and 4, respectively. The measurement geometry is shown as an inset in Fig. 4. The three characteristic surface states of the 7×7 surface [0.2, 0.8, and 1.7 eV below E_F (Ref. 23)] are not at all present on the Si(111)"7×1":H surface. Instead, a hydrogen-induced structure (labeled S) appears in the spectra. There are also two other distinct structures (labeled B_1 and B_2) in the spectra. S and B_1 are seen for emission angles larger than 25° along the $\bar{\Gamma}$-$\bar{K}$-$\bar{M}$ direction in the 1×1 SBZ, while along the $\bar{\Gamma}$-$\bar{M}$ direction they are seen also for an emission angle of 20°. The third distinct peak, B_2, is seen for small emission angles in the two main azimuthal directions.

The dispersions (initial energy versus k parallel) determined in this study for S, B_1, and B_2 are plotted, relative to the valence-band maximum, in Fig. 5. The Fermi-level position was 0.86 eV above the valence-band edge, for the unannealed surface as determined by measurements of the Si $2p$ core level. In the calculations of the dispersions a value of 4.73 eV was used for the work function. For the 7×7 surface the work function is assumed to be 4.63 eV, determined by Hollinger and Himpsel,[28] and according to Sakurai and Hagstrum[3] the work function has increased by ≈0.1 eV when the LEED pattern is transformed to the "7×1" pattern.

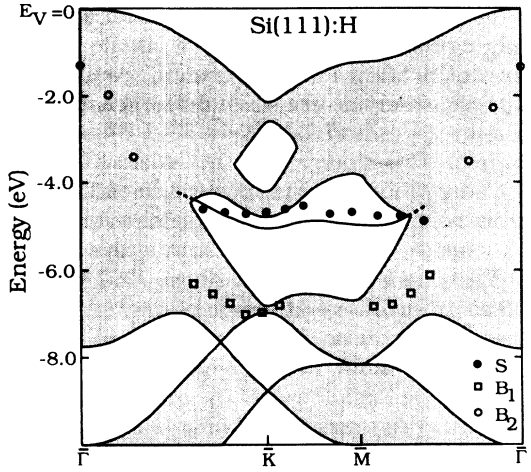

FIG. 5. Dispersion of the surface state originating from the Si—H bonds for the monohydride phase as calculated, by Pandey (Ref. 1) (solid curve). The surface-state dispersion determined in this study is shown by the dots. Also included are the dispersions for the bulk structures, which are shown as squares (B_1) and circles (B_2). The shaded regions are bulk energy bands projected on the 1×1 SBZ (Ref. 1).

The only true surface state, i.e., a state localized within a band gap, seen in this study is centered around -5.6 eV relative to E_F and it shows a small dispersion. This surface state originates from the Si—H bonds which are formed when the H atoms saturate the dangling bonds. As can be seen in Fig. 5 the surface-state dispersion is in good agreement with the calculated surface-state dispersion for the monohydride phase (solid curve in Fig. 5). It should be noted that S appears as a surface resonance near $\bar{K}$ and that close to $\bar{K}$ the structure B_2 has a similar dispersion (described below) as S, though B_2 is not seen in this region of k space for the "7×1":H surface.

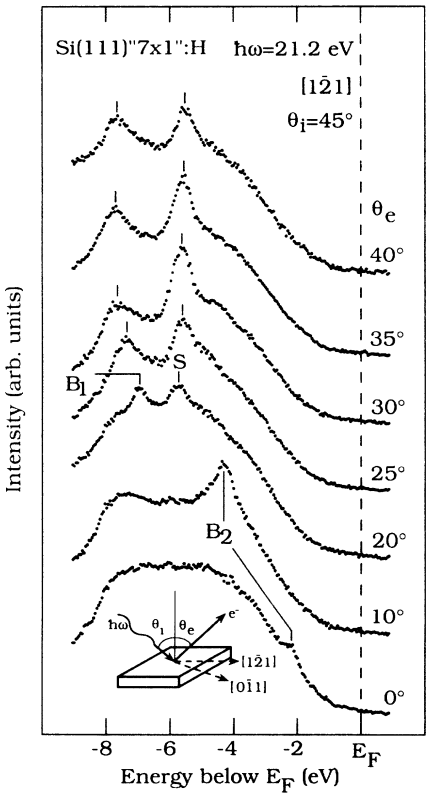

FIG. 4. Photoemission spectra recorded with 21.2 eV photon energy for various angles of emission along the $\bar{\Gamma}$-$\bar{M}$ direction in the 1×1 SBZ. The measurement geometry is shown as an inset.

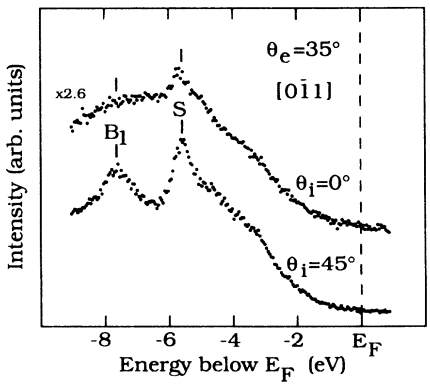

FIG. 6. Photoemission spectra recorded with 21.2 eV for two different incidence angles along the $\bar{\Gamma}$-$\bar{K}$-$\bar{M}$ direction in the 1×1 SBZ.

Pandey[1] predicted that the hydrogen-induced surface state for the monohydride phase should be visible only in a band gap near the 1×1 SBZ boundary. For the trihydride phase he predicted two hydrogen-induced states centered around ≈6 eV below E_V, which should be visible in the whole 1×1 SBZ. Since we observe only one surface state, just near the zone boundary and since the experimental surface-state dispersion is in good agreement with the calculated one for the monohydride phase we conclude that the monohydride phase exists within the 7×7 unit cell after the hydrogen exposure.

Structure B_2 has been reported earlier by Uhrberg *et al.*,[23] and it was shown that this structure is due to a direct bulk transition from the second topmost valence band. Uhrberg *et al.* compared the calculated dispersion, obtained by assuming a free-electron final band, with the experimental dispersion and found a very good agreement. The dispersion of B_2, obtained in this study, for the "7×1":H surface is in good agreement with the above-described dispersions, which proves that it is the same bulk transition.

Structure B_1 has previously been reported as a hydrogen-induced structure, i.e., an enhancement of a *sp*-like band.[3,5] It appeared in the angle-integrated spectra as a broad structure centered around ≈7.6 eV below E_F. This is explained by the fact that the dispersion for B_1 is quite small (see Fig. 5). The above-described analysis of direct bulk transitions, assuming a free-electron final band,[23] has been applied in this study also to B_1. The experimentally determined dispersion is in qualitative agreement with the calculated dispersion for a direct bulk transition from the second valence band (from the bottom). The assignment of B_1 to a direct bulk transition is further verified by the fact that B_1 is also seen in photoemission spectra from Si(111)7×7 and Si(111)$\sqrt{3}\times\sqrt{3}$:Al.[23]

Photoemission spectra recorded for different incidence angles, in order to further characterize the hydrogen-induced surface state, are shown in Fig. 6. There is a strong decrease in the emission intensity from the surface state when θ_i is changed from 45° to 0°, indicating that it is mainly the electric field perpendicular to the surface that is exciting the surface state. Therefore we conclude that the surface state has a substantial p_z character, which is expected for the monohydride phase. The intensity for B_1 is also highly reduced when $\theta_i = 0°$. This polarization dependence is observed for this peak also for the $\sqrt{3}\times\sqrt{3}$:Al surface.

IV. SUMMARY AND CONCLUSIONS

To summarize, measurements of the Si 2*p* core-level on the Si(111)7×7 and the Si(111)"7×1":H surfaces have been performed. In the interpretation of the result from these measurements we have used the DAS model for the 7×7 surface. Based on a charge-transfer argument and the observed intensities for the surface shifted components on the 7×7 surface we assign S_1 to the adatoms plus the atoms binding to the adatoms and S_2 to the rest atoms. With these assignments one arrives at the same explanation of the surface core-level shifts for both Si(111)7×7 and Ge(111)*c*(2×8) (Ref. 24).

In the Si 2*p* core-level spectrum of the Si(111)"7×1":H surface a surface component (S_1'), with a shift corresponding to Si atoms bonded to H atoms, is seen. The observed intensity decrease for S_1', as compared to S_1, can be explained if each adatom is replaced by three hydrogen atoms and if each rest atom dangling bond is saturated with a hydrogen atom. The formation of the monohydride phase is further evidenced by the fact that no components originating from the dihydride or the trihydride phase are seen and also by the result of the ARPES measurements on the hydrogen exposed surface.

We observe only one surface state in the ARPES spectra for the Si(111)"7×1":H surface, the dispersion of which is in good agreement with the one calculated for the monohydride phase.[1] For the trihydride phase Pandey[1] predicted two hydrogen-induced states in the same energy region and thus the observation of only one surface-state band excludes the trihydride phase. The surface state has a substantial p_z character which is expected for the monohydride phase.

The position of the Fermi level in the band gap is determined. For the 7×7 surface the Fermi-level pinning is the same for both the *n*- and the n^+-doped sample. For the annealed (≈400°C) "7×1":H surface the Fermi-level is determined to be 1.06 eV above the valence-band edge, assuming 0.63 eV (Ref. 25) for the 7×7 surface, which is close to the bulk value for the n^+-doped sample, thus indicating that the Fermi level is not pinned at the surface after the hydrogen exposure.

ACKNOWLEDGMENTS

The assistance of the Max-lab staff is gratefully acknowledged. This work was supported by the Swedish Natural Science Research Council.

[1]K. C. Pandey, Phys. Rev. B **14**, 1557 (1976); K. C. Pandey, IBM, J. Res. Develop. **22**, 250 (1978).
[2]H. Ibach and J. E. Rowe, Surf. Sci. **43**, 481 (1974).
[3]T. Sakurai and H. D. Hagstrum, Phys. Rev. B **12**, 5349 (1975).
[4]K. Fujiwara, Phys. Rev. B **26**, 2036 (1982).
[5]D. E. Eastman, F. J. Himpsel, J. A. Knapp, and K. C. Pandey, in *Physics of Semiconductors, 1978* Inst. Phys. Conf. Ser. No. 43 edited by B. H. Wilson (IOP, London, 1979), p. 1059.
[6]E. G. McRae and C. W. Caldwell, Phys. Rev. Lett. **46**, 1632 (1981).
[7]E. G. McRae, Surf. Sci. **147**, 663 (1984).
[8]A. Ichimiya and S. Mizuno, Surf. Sci. **191**, L765 (1987).
[9]H. Wagner, R. Butz, U. Backes, and D. Bruchmann, Solid State Commun. **38**, 1155 (1981).
[10]Y. J. Chabal, G. S. Higashi, and S. B. Christman, Phys. Rev. B **28**, 4472 (1983).
[11]T. Miller, T. C. Hsieh, and T.-C. Chiang, Phys. Rev. B **33**, 6983 (1986).
[12]K. Takayanagi, Y. Tanishiro, M. Takahashi, and S. Takahashi, J. Vac. Sci. Technol. A **3**, 1502 (1985).

[13]P. Mårtensson, Ph.D. thesis, Linköping University, 1986.
[14]U. O. Karlsson, J. N. Andersen, K. Hansen, and R. Nyholm, Nucl. Instrum. Methods A **282**, 553 (1989).
[15]A. Ishizaka and Y. Shiraki, J. Electrochem. Soc. **133**, 666, (1986).
[16]W. Eberhardt, G. Kalkoffen, C. Kunz, D.Aspnes, and M. Cardona, Phys. Status Solidi B **88**, 135 (1978).
[17]P. H. Mahowald, D. J. Friedman, G. P. Carey, K. A. Bertness, and J. J. Yeh, J. Vac. Sci. Technol. A **5**, 2982 (1987).
[18]J. F. Morar, U. O. Karlsson, J. A. Yarmoff, D. Rieger, F. R. McFeely, and F. J. Himpsel, National Synchrotron Light Source Annual Report 1986, Brookhaven National Laboratory, New York, 1986, p. 135 (unpublished).
[19]T.-C. Chiang, CRC Crit. Rev. Solid State Mater. Sci. **14**, 269 (1988).
[20]R. I. G. Uhrberg, G. V. Hansson, U. O. Karlsson, J. M. Nicholls, P. E. S. Persson, S. A. Flodström, R. Engelhardt, and E.-E. Koch, Phys. Rev. Lett. **52**, 2265 (1984).
[21]J. E. Northrup, Phys. Rev. Lett. **57**, 154 (1986).
[22]R. J. Hamers, R. M. Tromp, and J. E. Demuth, Phys. Rev. Lett. **56**, 1972 (1986).
[23]R. I. G. Uhrberg, G. V. Hansson, J. M. Nicholls, P. E. S. Persson, and S. A. Flodström, Phys. Rev. B **31**, 3805 (1985).
[24]J. Aarts, A.-J. Hoeven, and P. K. Larsen, Phys. Rev. B **38**, 3925 (1988).
[25]F. J. Himpsel, G. Hollinger, and R. A. Pollak, Phys. Rev. B **28**, 7014 (1983).
[26]R. Wolkow and Ph. Avouris, Phys. Rev. Lett. **60**, 1049 (1988).
[27]F. J. Himpsel, P. Heimann, T.-C. Chiang, and D. E. Eastman, Phys. Rev. Lett. **45**, 1112 (1980).
[28]G. Hollinger and F. J. Himpsel, J. Vac. Sci. Technol. A **1**, 640 (1983).
[29]C. U. S. Larsson, A. S. Flodström, R. Nyholm, L. Incoccia, and F. Senf, J. Vac. Sci. Technol. A **5**, 3321 (1987).
[30]L. S. O. Johansson (unpublished).

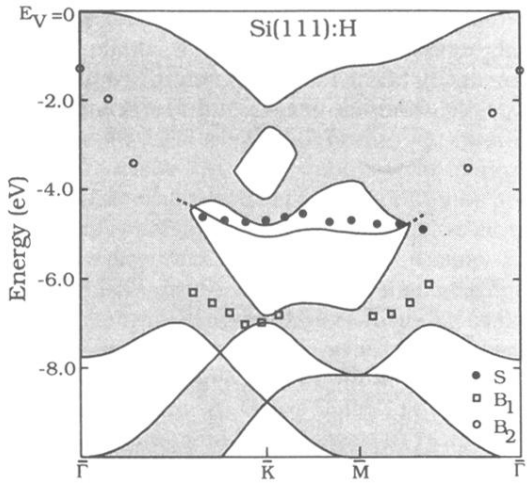

FIG. 5. Dispersion of the surface state originating from the Si—H bonds for the monohydride phase as calculated, by Pandey (Ref. 1) (solid curve). The surface-state dispersion determined in this study is shown by the dots. Also included are the dispersions for the bulk structures, which are shown as squares (B_1) and circles (B_2). The shaded regions are bulk energy bands projected on the 1×1 SBZ (Ref. 1).